Quantum trajectories in complex space

Chia-Chun Chou and Robert E. Wyatt*
Institute for Theoretical Chemistry and Department of Chemistry and Biochemistry, The University of Texas at Austin, Austin, Texas 78712, USA

(Received 8 April 2007; published 20 July 2007)

Quantum trajectories in complex space in the framework of the quantum Hamilton-Jacobi formalism are investigated. For time-dependent problems, the complex quantum trajectories determined from the exact analytical wave function for the free Gaussian wave packet and the coherent state in the harmonic potential are used to demonstrate that the information transported by the particles in the complex space can be used to synthesize the time-dependent wave function on the real axis. For time-independent problems, the exact complex quantum trajectories for the Eckart potential are obtained by numerically integrating the equations of motion. The unusual structure of the total potential (the sum of the classical and the quantum potentials) for the stationary states for the Eckart potential is pointed out. The variations of the complex-valued kinetic energy, classical potential, and quantum potential along the complex quantum trajectories are analyzed. This paper not only analyzes complex quantum trajectories for time-dependent and time-independent systems but also provides a unified description for complex quantum trajectories for one-dimensional problems in the quantum Hamilton-Jacobi formalism.

DOI: 10.1103/PhysRevA.76.012115 PACS number(s): 03.65.Ta, 03.65.Ca

I. INTRODUCTION

One of the several formulations of nonrelativistic quantum mechanics is Bohmian mechanics, developed by Bohm in 1952 [1]. The wave function is first written in terms of the *real* amplitude and the *real* action function as $\Psi = R\exp(iS/\hbar)$. Substituting this wave function in polar form into the time-dependent Schrödinger equation yields a system of two coupled partial differential equations, the continuity equation and the quantum Hamilton-Jacobi equation (QHJE). These are basic equations of quantum hydrodynamics. In Bohm's analytical approach, *real-valued* quantum trajectories are generated by integrating equations of motion including the contribution of the quantum potential determined from a precomputed wave function. Some physical processes such as atom diffraction by surfaces and the dissociation of molecules at metal surfaces have been studied by computing and interpreting real quantum trajectories through this analytical method [2,3]. On the other hand, new computational methods have been developed to compute real quantum trajectories and the wave function concurrently. The quantum trajectory method (QTM) has been introduced to integrate the hydrodynamic equations *on the fly* to generate the probability density by evolving ensembles of real quantum trajectories [4]. The QTM has been applied to model collinear reactions and to multidimensional wave packet scattering problems in Ref. [5], and the references cited therein. In addition, a related approach, the quantum fluid dynamics (QFD) has been developed to solve the same hydrodynamic equations [6]. Comprehensive exposition is presented in Holland's book [7] and recent developments of this formulation have been presented in Wyatt's book [5].

The quantum Hamilton-Jacobi formalism, developed by Leacock and Padgett in 1983, provides an alternative formulation of nonrelativistic quantum mechanics [8,9]. In this formalism, the wave function is expressed by the *complex* action function $\Psi = \exp(iS/\hbar)$. As in Bohmian mechanics, substituting the wave function in this polar form into the time-dependent Schrödinger equation yields the *complex-valued* QHJE (this version is not the same as that in Bohm's formalism). By separating out the time for stationary states, we obtain the stationary-state version of the QHJE. The main feature of this formalism is that the bound state energy eigenvalues can be determined by the quantum action variable without explicitly solving the dynamical equation. This method has been used to obtain the energy eigenvalues for many one-dimensional bound state problems and separable problems in higher dimensions for solvable potentials [8–11]. Furthermore, an accurate computational procedure for the complex-valued QHJE for one-dimensional bound state and scattering problems has been proposed by Chou and Wyatt to obtain the wave function and the reflection and transmission coefficients [12,13].

Besides the determination of energy eigenvalues, the quantum Hamilton-Jacobi formalism has been used to obtain quantum trajectories in the *complex* space. In Bohm's formalism, the particle is usually at rest for stationary states because the particle velocity turns out to be zero everywhere. On the contrary, the complex quantum trajectory of a particle can be obtained in the quantum Hamilton-Jacobi formalism for both stationary and nonstationary states through the quantum momentum function (QMF), which is extended to the complex space. John has applied this formalism to several simple analytical examples for time-dependent and time-independent problems [14]. In addition, for stationary states, complex quantum trajectories satisfying the complex-valued QHJE have been analytically studied for the free particle, the potential step, the potential barrier, the harmonic potential, and the hydrogen atom [14–21]. For nonstationary states, a simple analytical study for the free Gaussian wave packet has been presented [14], and a computational method has

*wyattre@mail.utexas.edu

been developed to obtain the *complex* quantum trajectories, the wave function, and tunneling probabilities for the scattering of a Gaussian wave packet from an Eckart barrier [22].

In recent studies by Rowland and Wyatt, the real-valued and complex-valued derivative propagation methods have been applied to one-dimensional and multidimensional scattering problems employing either Eckart or Gaussian barriers [23,24]. Deep tunneling and higher energy barrier transmission probabilities were compared with the exact results. The dynamics of the complex quantum trajectories and the properties of the complex-extended barrier potentials were described and analyzed in detail. It was found that barrier transmission probabilities obtained using a low-order derivative propagation method and even classical complex trajectories are in excellent agreement with the exact results.

A significant difference between the quantum Hamilton-Jacobi formalism and the conventional Bohmian mechanics is that the quantum trajectory of a particle can be obtained in the quantum Hamilton-Jacobi formalism for both stationary and nonstationary states, while the particle is usually at rest for stationary states in Bohmian mechanics. In addition, the relationship of the quantum potential between these two formalisms has been presented in the Appendix of Ref. [12]. The equations of motion for real-valued and complex-valued quantum trajectories have been compared in the Appendix of Ref. [23]. A brief comparison of the quantum Hamilton-Jacobi formalism with Bohmian mechanics has been presented, and the necessity of extending quantum trajectories to complex space has been discussed by Yang [15,21].

On the other hand, the extension of classical trajectories to the complex space have been applied to a diverse range of physical problems. For example, complex classical trajectories have been used to calculate the S matrix in reactive molecular collisions [25–27]. The propagation of Gaussian wave packets has been extended into the complex phase space [28–30]. A WKB-type procedure of semiclassical propagation of wave packets using classical trajectories evolving in complex phase space has been proposed [31].

The purpose of this paper is to present a *unified description* of quantum trajectories in the complex space for time-dependent and time-independent problems. The equations of motion for complex quantum trajectories for time-dependent and time-independent problems are connected in the framework of the quantum Hamilton-Jacobi formalism. For time-dependent problems, we present analytical studies for quantum trajectories in the complex space through two exactly solvable problems. In these examples, the particles transport information such as the complex action along the complex quantum trajectories. The information transported by particles crossing the real axis simultaneously can be used to synthesize the wave function. Here, the concept of "isochrone" will be used. That means that the particles launched from a specific isochrone will arrive at the real axis simultaneously. The concept behind isochrone has been used for the scattering of a Gaussian wave packet [22], and the term "isochrone" has been introduced and described in Refs. [23,24]. For time-independent problems, we demonstrate complex quantum trajectories obtained numerically by either forward or backward integrations for the Eckart potential. Additionally, the unusual and complicated structure of the state-dependent total potential (the classical and the quantum potentials) is presented. The variations of the kinetic energy, the classical potential, and the quantum potential along the complex quantum trajectory for stationary states are analyzed. In the backward integration, we find that some complex quantum trajectories spiral into attractors in the barrier region.

This paper is organized as follows: We begin by deriving the equations of motion for complex quantum trajectories for time-dependent problems in Sec. II. In Sec. III, analytical studies for the complex quantum trajectories for the free Gaussian wave packet and the coherent state in the harmonic potential are presented. It is also described how the particles launched from the isochrone transport the complex action to the real axis to obtain the time-dependent wave function. In Sec. IV, the equations of motion for complex quantum trajectories for time-independent problems are derived. In addition, the difficulties to solve time-dependent and time-independent problems are compared. In Sec. V, some remarks for bound state problems are made, and numerical studies for complex quantum trajectories scattering from the Eckart potential are presented. Finally, we make some comments and conclude with a discussion about future research directions for complex quantum trajectories.

II. EQUATIONS OF MOTION FOR QUANTUM TRAJECTORIES: TIME-DEPENDENT PROBLEMS

The Hamilton-Jacobi formulation of quantum mechanics was proposed by Leacock and Padgett in 1983 [8,9]. The complex-valued QHJE is readily obtained by substituting the polar form of the complex-valued wave function,

$$\Psi(x,t) = \exp\left[\frac{i}{\hbar}S(x,t)\right], \tag{1}$$

into the time-dependent Schrödinger equation to obtain

$$-\frac{\partial S}{\partial t} = \frac{1}{2m}\left(\frac{\partial S}{\partial x}\right)^2 + V(x) + \frac{\hbar}{2mi}\frac{\partial^2 S}{\partial x^2}, \tag{2}$$

where $S(x,t)$ is the complex action, and this equation is described in Tannor's book [32]. As in Bohmian mechanics, the QMF is given by the guidance equation $p(x,t)=\partial S(x,t)/\partial x$. In order to find a quantum trajectory, we may rearrange this equation as

$$\frac{dx}{dt} = \frac{1}{m}\frac{\partial S(x,t)}{\partial x}. \tag{3}$$

However, since the action $S(x,t)$ is complex valued and time remains real valued, the trajectory requires a complex-valued coordinate. Therefore, the QMF $p(x,t)$ and the complex action $S(x,t)$ are extended to the complex space by regarding x as a complex variable. Thus, a complex quantum trajectory is defined by

$$\frac{dz}{dt} = \frac{p(z,t)}{m}, \tag{4}$$

where x has been replaced by a complex variable z (the complex variable will be denoted by $z=x+iy$, where x and y are

the real and imaginary parts, respectively). In addition, the first, second, and third terms on the right side of Eq. (2) correspond to the kinetic energy, the classical potential, and the quantum potential in the complex space, respectively.

Through Eq. (2), we can obtain the equations of motion for $z(t)$, $p(z,t)$, and $S(z,t)$ for quantum trajectories in the complex space

$$\frac{dz}{dt} = \frac{p}{m}, \tag{5}$$

$$\frac{dp}{dt} = \frac{\partial p}{\partial z}\frac{dz}{dt} + \frac{\partial p}{\partial t} = -\frac{dV(z)}{dz} - \frac{\hbar}{2mi}\frac{\partial^2 p}{\partial z^2}, \tag{6}$$

$$\frac{dS}{dt} = \frac{\partial S}{\partial z}\frac{dz}{dt} + \frac{\partial S}{\partial t} = \frac{p^2}{2m} - V(z) - \frac{\hbar}{2mi}\frac{\partial p}{\partial z}. \tag{7}$$

These equations of motion have been described and applied by Tannor and co-workers [22]. Therefore, we can determine the quantum trajectories of particles in the complex space by integrating these equations and the wave function can be synthesized by Eq. (1).

For time-dependent problems, the initial state $\Psi(z,0)$ is used to determine the initial condition $(z_0, p(z_0,0), S(z_0,0))$ where z_0 is the starting point of the trajectory. Additionally, we can also find that the integration of the equations of motion involves the spatial derivative for $p(z,t)$. Therefore, the equations of motion are not closed and general numerical methods for a system of ordinary differential equations cannot be applied to the integration of the equations of motion for quantum trajectories. However, the derivative propagation method (DPM) has been developed to overcome a similar difficulty in Bohmian mechanics by solving a truncated system of equations for amplitude, phase, and their spatial derivatives [33]. Through use of the DPM, a computational approach for solving the equations of motion in the complex space using the iteration of the spatial partial derivatives of $p(z,t)$ has been developed recently by Tannor and coworkers [22].

We can obtain quantum trajectories in the complex space with arbitrary initial positions, and the initial conditions for the quantum trajectories are determined by the initial state. Namely, a particle can start its motion at any position and it will transport information such as the complex action along the complex quantum trajectory. When the particle crosses the real axis, we can record the information. Thus, for those particles which cross the real axis simultaneously, the wave function on the whole real axis can be synthesized using the information transported by these particles. Because the correct wave function at a specific time on the real axis must be determined by the information transported by particles arriving simultaneously at the real axis, we define a curve for the special initial positions of these particles in the complex space as an "isochrone." The concept and use of isochrones have been applied in Refs. [22–24]. In the following section, these concepts will be demonstrated.

III. TIME-DEPENDENT EXAMPLES

In this section, we will present analytical studies for exact complex quantum trajectories and two exact solvable systems will be examined thoroughly.

A. Gaussian wave packet

We now consider a free Gaussian wave packet with a momentum $\hbar k_0$. The wave packet is given initially by a normalized Gaussian centered at the origin with a plane wave component as follows:

$$\Psi(x,0) = \frac{1}{(\pi L^2)^{1/4}} e^{-x^2/2L^2} e^{ik_0 x}. \tag{8}$$

The exact time-dependent wave packet is given analytically [34] by

$$\Psi(x,t) = \frac{1}{(\pi L^2)^{1/4}} \frac{1}{(1+i\hbar t/mL^2)^{1/2}} e^{i[k_0 x - (\hbar k_0^2/2m)t]} \times e^{-(x-\hbar k_0 t/m)^2/[2L^2(1+i\hbar t/mL^2)]}. \tag{9}$$

Substituting this wave function into the definition of the QMF in the complex space gives

$$p(z,t) = \frac{\hbar}{i}\frac{1}{\Psi(z,t)}\frac{\partial \Psi(z,t)}{\partial z} = \frac{\hbar}{i}\left(ik_0 - \frac{z-\hbar k_0 t/m}{L^2(1+i\hbar t/mL^2)}\right), \tag{10}$$

where z is a complex variable. Similarly, the quantum and total potentials are easily determined by

$$Q(z,t) = \frac{\hbar}{2mi}\frac{\partial p(z,t)}{\partial z} = \frac{\hbar^2}{2}\frac{1}{i\hbar t + mL^2}, \tag{11}$$

$$V_{\text{tot}}(z,t) = V(z) + Q(z,t) = \frac{\hbar^2}{2}\frac{1}{i\hbar t + mL^2}, \tag{12}$$

where $V(z)=0$ in this problem. The quantum and total potentials are independent of position and depend only upon the time.

Because we start with the analytical form of the wave function, the spatial partial derivatives in Eqs. (5)–(7) can be expressed analytically in terms of z and t. Thus, the set of the equations of motion for quantum trajectories becomes closed and the equations of motion in the complex space are given by

$$\frac{dz}{dt} = \frac{\hbar(z - ik_0 L^2)}{\hbar t - imL^2}, \tag{13}$$

$$\frac{dp}{dt} = 0, \tag{14}$$

$$\frac{dS}{dt} = \frac{\hbar^2[m(iz + k_0 L^2)^2 - (i\hbar t + mL^2)]}{2(i\hbar t + mL^2)^2}, \tag{15}$$

where Eq. (13) has been presented in Ref. [14]. From Eq. (14), we note that the classical and the quantum forces are all

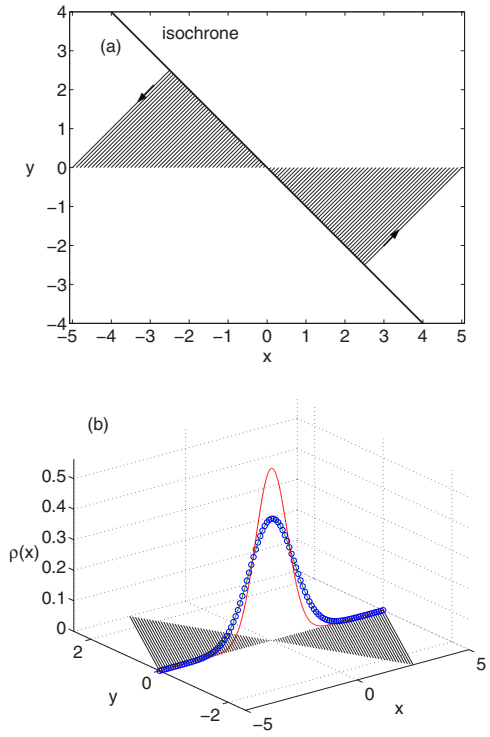

FIG. 1. (Color online) Nontranslating free Gaussian wave packet ($k_0=0$): (a) Complex quantum trajectories starting from the isochrone arrive at the real axis at $t=1$; (b) Complex quantum trajectories (black curves) on the complex plane; probability densities of the Gaussian wave packet: $t=0$ (red curve); $t=1$ (exact) (green curve); $t=1$ (numerical) [blue circles (○)].

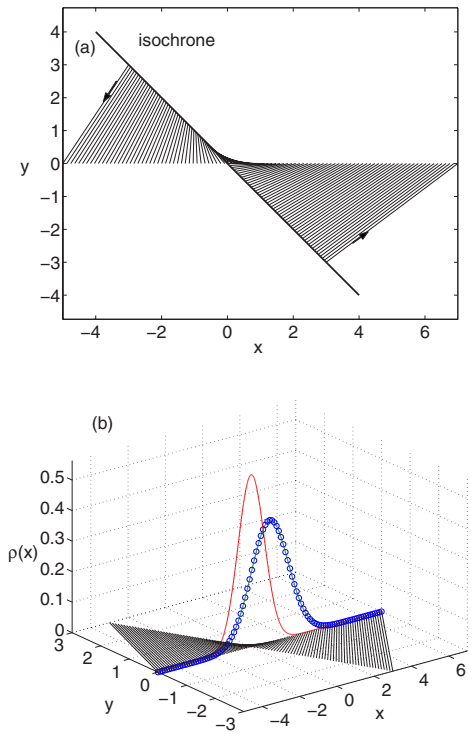

FIG. 2. (Color online) Translating free Gaussian wave packet ($k_0=1$): (a) Complex quantum trajectories starting from the isochrone arrive at the real axis at $t=1$; (b) complex quantum trajectories (black curves) on the complex plane; probability densities of the Gaussian wave packet: $t=0$ (red curve); $t=1$ (exact) (green curve); $t=1$ (numerical) [blue circles (○)].

equal to zero. The initial conditions for the equations of motion with an arbitrary initial position z for a complex quantum trajectory $(z,p(z,0),S(z,0))$ are determined by the initial state given in Eq. (8). Therefore, $p(z,0)$ and $S(z,0)$ are given by

$$p(z,0) = \frac{\hbar}{i}\frac{1}{\Psi(z,0)}\frac{\partial\Psi(z,0)}{\partial z} = \hbar k_0 - \frac{\hbar z}{iL^2}, \tag{16}$$

$$S(z,0) = \frac{\hbar}{i}\ln\Psi(z,0) = \frac{i\hbar z^2}{2L^2} + \hbar k_0 z + \frac{i\hbar}{4}\ln(\pi L^2). \tag{17}$$

The last term of Eq. (17) comes from the normalization constant of the initial Gaussian wave packet given by Eq. (8), and it actually can be dropped because the wave function synthesized at later times from Eq. (1) can be renormalized.

In this example, the equation of motion for the complex quantum trajectory given by Eq. (13) can be analytically solved and the exact solution is given by

$$z(t) = \frac{\hbar t}{mL^2}(iz_0 + k_0L^2) + z_0, \tag{18}$$

where z_0 is the starting point at $t=0$, and this solution has been presented in Ref. [14].

The isochrone equation can be determined by setting $\mathrm{Im}[z(t)]=0$, and it is given by

$$\frac{x_0\hbar t}{mL^2} + y_0 = 0, \tag{19}$$

where x_0 and y_0 are the real and the imaginary parts of the starting point z_0. From this equation, we find that if a particle starts its motion with an initial position (x_0,y_0), then the imaginary part of its position will become zero at $t=-y_0mL^2/x_0\hbar$ and this means that the particle arrives at the real axis. Therefore, the arrival time t_A is proportional to the slope of the isochrone as follows:

$$t_A = -\frac{mL^2}{\hbar}\frac{y_0}{x_0}. \tag{20}$$

The system of the equations of motion given by Eqs. (13)–(15) is closed; therefore, general numerical methods for differential equations can be used. The complex quantum trajectories and the probability densities are shown in Figs. 1 and 2. All the relevant physical quantities will be used in the following dimensionless units: $\bar{z}=z/L$, $\bar{k}_0=k_0/(1/L)$, $\bar{t}=t/(mL^2/\hbar)$, $\bar{p}=p/(\hbar/L)$, $\bar{S}=S/\hbar$, and $\bar{V}=V/(\hbar^2/mL^2)$. We will denote the value of a given dimensionless physical quantity with the same symbol as the quantity itself. The quantum trajectories were determined using the fourth-order Runge-Kutta integration method and the initial conditions given by Eqs. (16) and (17) with the time step size $\Delta t=0.1$. First, we consider a special case with $k_0=0$: a nontranslating

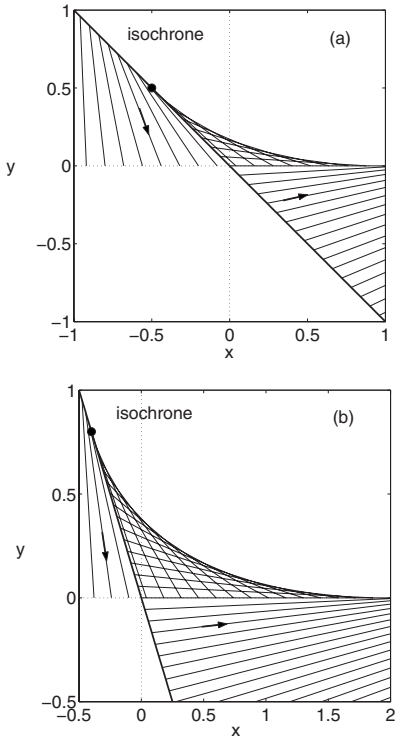

FIG. 3. Translating free Gaussian wave packet ($k_0=1$): (a) Complex quantum trajectories starting from the isochrone (thick black line) arrive at the real axis at $t=1$; (b) complex quantum trajectories starting from the isochrone (thick black line) arrive at the real axis at $t=2$. The bifurcation points z_b are also shown (●).

Gaussian wave packet. From Eqs. (19) and (20), we know that the isochrones are straight lines and the arrival time is just the negative sign of the slope. Figure 1(a) shows that the particles on the isochrone will arrive at the real axis at $t=1$. The information such as positions and complex actions that they transport can be used to synthesize the wave function at $t=1$ along the real axis. For general cases, since the numerically obtained final positions of the particles may be not exactly on the real axis, interpolation can be used to approximate the complex action values [22]. In Fig. 1(b), the synthesized probability density at $t=1$ is in excellent agreement with the exact result. Additionally, this figure shows the spreading of the probability density of the Gaussian wave packet with a peak value that decreases in time. Subsequently, we consider a translating Gaussian wave packet with $k_0=1$. Figure 2(a) shows that the particles on the isochrone arrive at the real axis at $t=1$. In Fig. 2(b), the synthesized probability density at $t=1$ is in excellent agreement with the exact result. Additionally, this figure shows the translation and the spreading of the Gaussian wave packet in time.

Furthermore, Fig. 3 shows the quantum trajectories in the vicinity of the origin in Fig. 2(a) and also the quantum trajectories starting on the isochrone with the slope equal to −2. For a nontranslating Gaussian wave packet, the particles launched from the isochrone on the left side of the imaginary axis will arrive at the left side of the real axis. Correspondingly, the particles launched from the isochrone on the right side of the imaginary axis will arrive at the right side of the real axis. Additionally, the particle starting at the origin will remain static. Differing from those complex quantum trajectories for the nontranslating free Gaussian wave packet shown in Figs. 1(a), some of the complex quantum trajectories starting on the left side of the imaginary axis shown in Fig. 3 can pass the imaginary axis to reach the real axis. This phenomenon reflects the translation to the right of the wave packet. Moreover, because the particle starting at the bifurcation point z_b (see Fig. 3) will arrive at the origin at $t=t_A$, we can determine this point as a function of the arrival time t_A by setting the trajectory equation given in Eq. (18) to be zero. Thus, the bifurcation point is given by

$$z_b(t_A) = -\frac{k_0 L^2}{i + mL^2/\hbar t_A}. \tag{21}$$

For the nontranslating Gaussian wave packet ($k_0=0$), $z_b(t_A)=0$ for any arrival time and the bifurcation point remains at the origin. For the translating Gaussian wave packet ($k_0=1$), the bifurcation point is $z_b=-1/2+i/2$ for $t_A=1$ and $z_b=-2/5+4i/5$ for $t_A=2$. These points are shown in Fig. 3.

B. Gaussian wave packet in a harmonic potential: Coherent state

We subsequently consider a more complicated example: a Gaussian wave packet in the harmonic potential $V(x)=(1/2)m\omega^2x^2$. The time-dependent Schrödinger equation for this system can be solved analytically for the exact solution [35] as follows:

$$\Psi(x,t) = N\exp\left[-\frac{\alpha^2}{2}\left(x - \frac{ip_0}{\hbar\alpha^2}\cos\omega t\right)^2 + \frac{p_0 x}{\hbar}\sin\omega t - \frac{i\omega t}{2} - \frac{ip_0^2}{4\hbar^2\alpha^2}\sin 2\omega t\right], \tag{22}$$

with an initial Gaussian wave packet centered at the origin

$$\Psi(x,0) = N\exp\left[-\frac{\alpha^2}{2}\left(x - \frac{ip_0}{m\omega}\right)^2\right], \tag{23}$$

where the prefactor N is the normalization constant and $\alpha^2=m\omega/\hbar$.

From the solution given by Eq. (22), we can obtain the QMF and then the equations of motion can be expressed by

$$\frac{dz}{dt} = \frac{e^{-i\omega t}p_0 + im\omega z}{m}, \tag{24}$$

$$\frac{dp}{dt} = -m\omega^2 z, \tag{25}$$

$$\frac{dS}{dt} = -\frac{1}{2}\frac{(m\omega z - ip_0 e^{-i\omega t})^2}{m} - \frac{1}{2}m\omega^2 z^2 - \frac{\hbar\omega}{2}. \tag{26}$$

From Eq. (25), we find that the term on the right side comes from the classical force and the quantum force is actually equal to zero. Additionally, the quantum potential $Q(z,t)=\hbar\omega/2$ and is equal to the ground state energy of the har-

monic oscillator. To numerically integrate the equations of motion, we need the initial conditions $(z,p(z,0),S(z,0))$ determined from Eq. (23),

$$p(z,0) = im\omega\left(z - \frac{ip_0}{m\omega}\right), \tag{27}$$

$$S(z,0) = \frac{(p_0 + im\omega z)^2}{2im\omega}, \tag{28}$$

where the constant term of Eq. (28) has been dropped.

The quantum trajectory equation given in Eq. (24) can be analytically solved and the exact quantum trajectory with an arbitrary starting point z_0 is given by

$$z(t) = \frac{p_0}{m\omega}\sin\omega t + z_0 e^{i\omega t}. \tag{29}$$

Similarly, the isochrone equation determined by setting the imaginary part of Eq. (29) to be zero is then given by

$$x_0 \sin\omega t + y_0 \cos\omega t = 0. \tag{30}$$

Again, the isochrone is a straight line. Furthermore, the arrival time for particles launched from an arbitrary isochrone to reach the real axis is

$$t_A = \frac{1}{\omega}\tan^{-1}\left[-\frac{y_0}{x_0}\right]. \tag{31}$$

In this case, the arrival time is a function of the slope of the isochrone.

In this example, all the relevant physical quantities will be used in the following dimensionless units: $\bar{z}=z/\sqrt{\hbar/m\omega}$, $\bar{t}=t/(1/\omega)$, $\bar{p_0}=p_0/(\sqrt{\hbar m\omega})$, $\bar{p}=p/(\sqrt{\hbar m\omega})$, $\bar{S}=S/\hbar$, and $\bar{V}=V/(\hbar\omega)$. We will denote the value of a given dimensionless physical quantity with the same symbol as the quantity itself. The complex quantum trajectories and the probability densities obtained by numerically solving the equations of motion (using the fourth-order Runge-Kutta method with the time step size $\Delta t=0.1$) are shown in Figs. 4 and 5. From Eqs. (30) and (31), we know that the isochrones are straight lines and if a particle starts its motion with an initial position (x_0,y_0), then it will reach the real axis at the arrival time t_A. Figure 4(a) shows that the particles on the isochrone with the slope equal to $-\tan 2$ at $t=0$ will arrive at the real axis at $t=2$. Again, we can see from Fig. 4(b) the synthesized probability density at $t=2$ is in excellent agreement with the exact result and the Gaussian wave packet moves to the right. Figure 5 shows that the particles on the isochrone with the slope equal to $-\tan 4$ at $t=0$ will arrive at the real axis at $t=4$, and the Gaussian wave packet moves to the left. If we continue to record the information of particles as they cross the real axis, the synthesized Gaussian wave packet will oscillate back and forth and maintain its width in time. In this example, the Gaussian wave packet is a coherent state and it oscillates without spreading. Moreover, Fig. 6 shows the quantum trajectories in the vicinity of the origin in Figs. 4(a) and 5(a). The particles starting on the isochrone show complicated

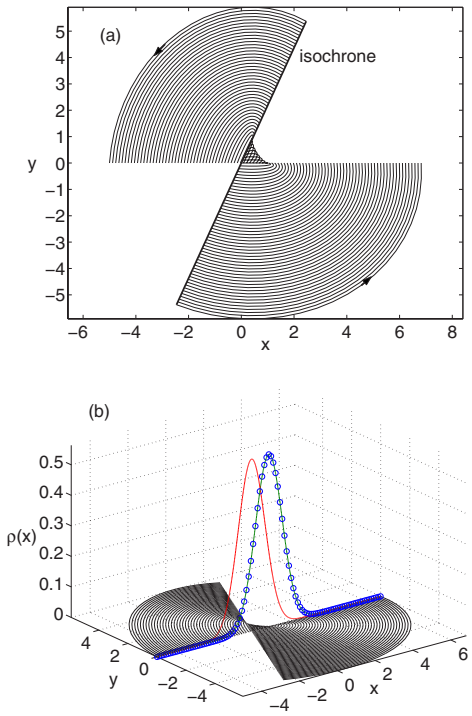

FIG. 4. (Color online) Coherent state: (a) Complex quantum trajectories starting from the isochrone (thick black line) arrive at the real x axis at $t=2$; (b) complex quantum trajectories (black curves) on the complex plane; probability densities of the Gaussian wave packet: $t=0$ (red curve); $t=2$ (exact) (green curve); $t=2$ (numerical) [blue circles (○)].

motion to reach the real axis. The arrows in Fig. 6 show the direction of these particles moving from the isochrone to the real axis.

Similarly, the bifurcation point determined by setting the trajectory equation given in Eq. (29) to be zero is given by

$$z_b(t_A) = -\frac{p_0}{m\omega}\sin\omega t_A e^{-i\omega t_A}. \tag{32}$$

As shown in Fig. 6, the particles starting on the isochrone from two different sides of the bifurcation point will arrive at the corresponding sides of the real axis. In particular, the particle starting at the bifurcation point shows a linear motion along the isochrone to the origin.

IV. EQUATIONS OF MOTION FOR QUANTUM TRAJECTORIES: TIME-INDEPENDENT PROBLEMS

In previous sections, the equations of motion and two examples for time-dependent problems have been presented and analyzed. We now consider time-independent problems. For stationary states with eigenenergy E, the complex action can be reexpressed by $S(z,t)=W(z)-Et$ and the QMF becomes

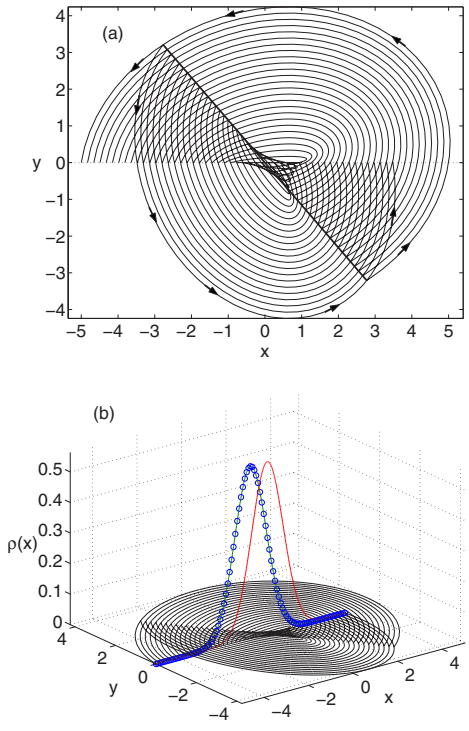

FIG. 5. (Color online) Coherent state: (a) Complex quantum trajectories starting from the isochrone (thick black line) arrive at the real x axis at $t=4$; (b) complex quantum trajectories (black curves) on the complex plane; probability densities of the Gaussian wave packet: $t=0$ (red curve); $t=4$ (exact) (green curve); $t=4$ (numerical) [blue circles (○)].

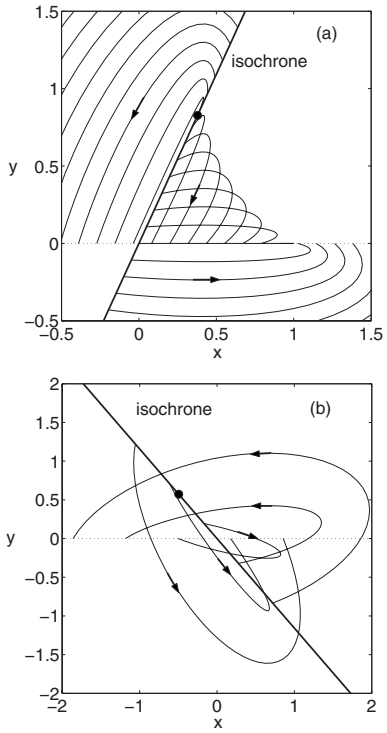

FIG. 6. Coherent state: (a) Complex quantum trajectories starting from the isochrone (thick black line) arrive at the real x axis at $t=2$; (b) complex quantum trajectories starting from the isochrone (thick black line) arrive at the real x axis at $t=4$. The bifurcation points z_b are also shown (●).

$$p(z,t) = \frac{\partial S}{\partial z} = \frac{dW(z)}{dz} = \bar{p}(z), \tag{33}$$

where $W(z)$ is called the quantum characteristic function and $\bar{p}(z)$ has been used to denote the stationary-state QMF. Moreover, the stationary-state QMF is related to the stationary-state wave function by

$$\bar{p}(z) = \frac{\hbar}{i}\frac{1}{\psi(z)}\frac{d\psi(z)}{dz}. \tag{34}$$

Then, using the expression $S(z,t)=W(z)-Et$ and rewriting the QHJE in Eq. (2) in terms of the stationary-state QMF yield the stationary-state QHJE

$$\frac{1}{2m}\bar{p}(z)^2 + V(z) + \frac{\hbar}{2mi}\frac{d\bar{p}(z)}{dz} = E. \tag{35}$$

Similarly, we can obtain the equations of motion for stationary states from Eqs. (5)–(7),

$$\frac{dz}{dt} = \frac{\bar{p}}{m}, \tag{36}$$

$$\frac{d\bar{p}}{dt} = \frac{2i}{\hbar}\left[E - V(z) - \frac{\bar{p}^2}{2m}\right]\bar{p}, \tag{37}$$

$$\frac{dW}{dt} = \frac{\bar{p}^2}{m}, \tag{38}$$

where the stationary-state QHJE in Eq. (35) has been used. Equations (36) and (37) have been described and applied by Yang [19].

When solving equations of motion for quantum trajectories, we will encounter different difficulties for time-dependent and time-independent problems, respectively. For time-dependent problems, the system of equations of motion given in Eqs. (5)–(7) is not closed because the QMF is coupled to its spatial derivative. Therefore, general numerical methods for differential equations cannot be applied directly. For time-independent problems, although the system of equations of motion given in Eqs. (36)–(38) is closed, it is evident from Eq. (34) that only solving the equations of motion with the *correct* initial quantum momentum $\bar{p}(z_0)$ can yield the *correct* quantum trajectories belonging to the corresponding stationary states. Moreover, it is found that from Eqs. (36)–(38) the quantum characteristic function $W(z)$ is not coupled to z and the QMF $\bar{p}$. Therefore, we only need to use Eqs. (36) and (37) to solve for quantum trajectories. In addition to determining quantum trajectories, we want to obtain the wave function along the real axis. A computational method for time-independent one-dimensional bound and scattering state systems has been developed to obtain the wave function along the real axis [12,13]. In summary, the

difficulty to solve time-dependent problems arises from the integration of the equations of motion, while the the difficulty to solve time-independent problems arises from the specification of the initial conditions.

V. TIME-INDEPENDENT EXAMPLES

In this section, two time-independent examples will be presented for bound and scattering state systems. For bound state problems, the harmonic oscillator will be used to illustrate the difficulty encountered when we solve for the complex quantum trajectories. For scattering-state problems, we will determine the complex quantum trajectories for the Eckart potential by either forward or backward integrations.

A. Bound states: Harmonic oscillator

The quantum trajectories in the complex space in a given quantum state have been explored analytically for the free particle, the harmonic potential, the potential step, the potential barrier, and the hydrogen atom [14–19]. Starting with the eigenfunction, we can determine the stationary-state QMF directly from Eq. (34). Then, the problem is reduced to solving Eq. (36) for complex quantum trajectories numerically or analytically. For the harmonic oscillator, the complex quantum trajectories for the ground and the first-excited states have been obtained in an analytical form, and general properties of the quantum harmonic oscillator in the complex space have been thoroughly studied [14,19].

For general bound state problems, it will be difficult to synthesize the wave function along the real axis from the information transported by particles if we cannot make a good approximation to the initial condition when solving the equations of motion for complex quantum trajectories. For time-independent problems, the stationary-state QMF and the quantum characteristic function are only a function of z. Namely, when particles evolve in the complex space with time, the QMF and relevant functions depend only on their positions, not on time. For the harmonic potential $V(x)=(1/2)m\omega^2x^2$, the quantum trajectories and the probability densities for the ground and the first-excited states are shown in Fig. 7. Here, the relevant physical quantities are used in the dimensionless units: $\bar{z}=z/(\sqrt{\hbar/m\omega})$, $\bar{p}=p/(\sqrt{\hbar m\omega})$, $\bar{t}=t/(1/\omega)$, and $\bar{E}=E/(\hbar\omega)$. We denote the value of a given dimensionless physical quantity with the same symbol as the quantity itself. Although particles propagate in the complex space, the values of their QMFs and relevant functions are actually determined by their positions. As we can see from Fig. 7, the probability densities do not change in time. Therefore, we do not need to use the same method for time-dependent problems to synthesize the wave function by starting from the isochrone, and we can synthesize the bound state wave function along the real axis as long as we can obtain the stationary-state QMF or the quantum characteristic function along the real axis. An accurate computational method to obtain both the QMF and the wave function along the real axis for one-dimensional bound state problems from the stationary-state QHJE has been developed, and it has also been applied to the harmonic oscillator and the Morse potential [12].

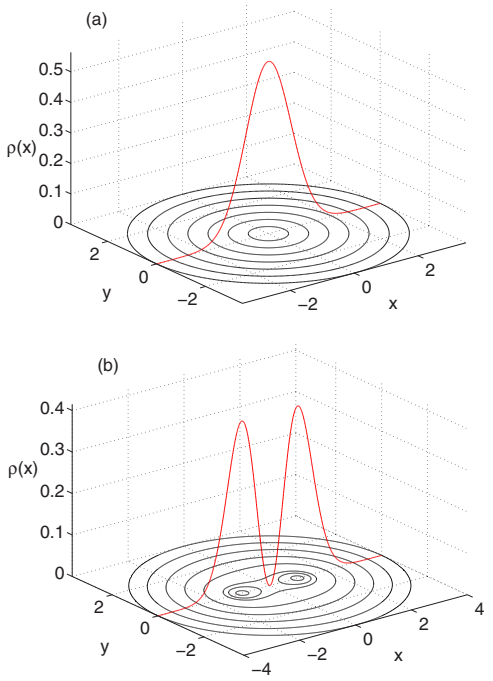

FIG. 7. (Color online) Complex quantum trajectories (black curves) and probability density (red curve) for the harmonic oscillator: (a) ground state; (b) first-excited state.

In addition, the quantum trajectories for the first-excited state of the harmonic oscillator are shown in Fig. 8. There are two types of complex quantum trajectories. One is the *localized* trajectory enclosing only one of the two equilibrium points on the real axis. If a particle starts its motion at the equilibrium point, it will remain static at the position. Thus, equilibrium points are special points. The information such as the complex action at equilibrium points cannot be transported to other positions by particles, and similarly, particles launched from other positions cannot transport their information to equilibrium points. The other is the *delocalized* trajectory enclosing all of the equilibrium points on the

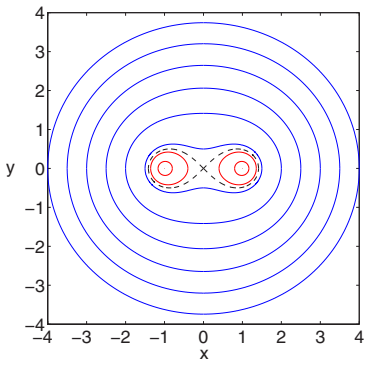

FIG. 8. (Color online) Complex quantum trajectories for the first-excited state of the harmonic oscillator and the bifurcation curve (---), which separates localized (red) and delocalized (blue) trajectories.

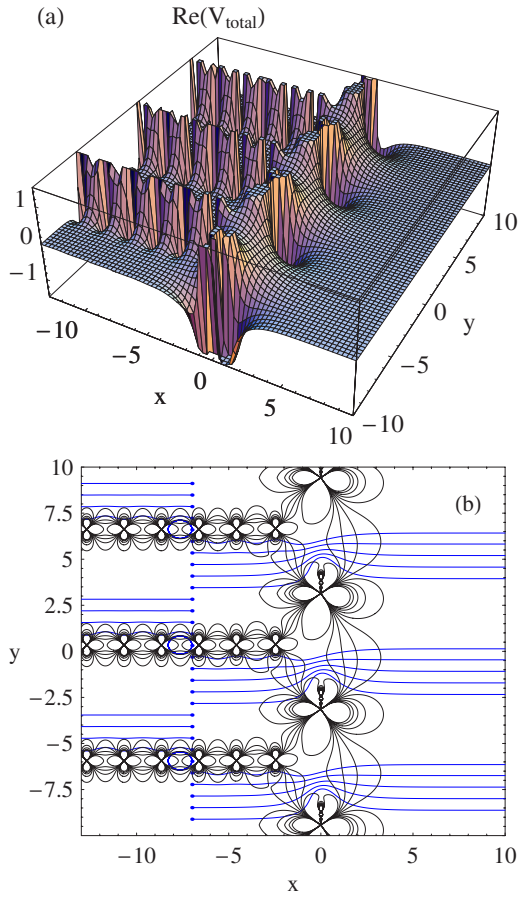

FIG. 9. (Color online) Forward integration for $E=1.2$, $V_0=1$: (a) Real part of the total potential; (b) quantum trajectories (blue curves) and the contour map of the real part of the total potential (black curves). The initial positions are shown as blue dots.

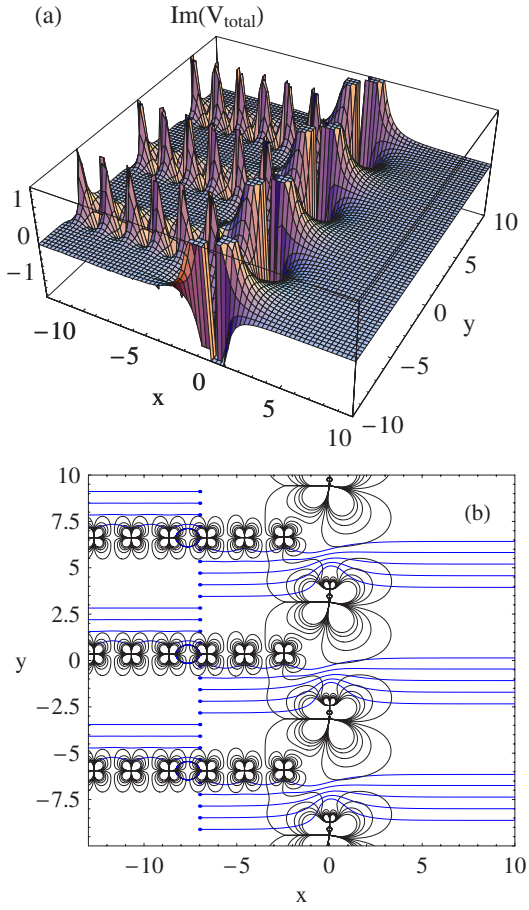

FIG. 10. (Color online) Forward integration for $E=1.2$, $V_0=1$: (a) Imaginary part of the total potential; (b) quantum trajectories (blue curves) and the contour map of the imaginary part of the total potential (black curves). The initial positions are shown as blue dots.

real axis. Furthermore, the origin is a singularity, which is the pole of the QMF corresponding to the node of the wave function, and it is undefined for the QMF. These two types of the trajectory are separated by the *bifurcation curve*, which is also shown (dashed line) in Fig. 8. The complex quantum trajectories for other excited states show the same structure. Detailed analysis of the complex quantum trajectories for the harmonic oscillator can be found in Refs. [14,19].

B. Scattering states: Eckart potential

We now present complex quantum trajectories for stationary states with eigenenergy E for the Eckart potential, which is given by $V(x)=V_0\,\mathrm{sech}^2(x/2a)$. The exact scattering wave function with energy E can be determined analytically [36],

$$\psi(x)=(-1)^{if}(2s)^{-1/2}\exp(-\pi f)w^{-if}(1-w)^{(is+if)}\times {}_2F_1((1/2 - if - ig - is),(1/2 - if + ig - is),(1-2is);(1-w)^{-1}),$$

where ${}_2F_1$ is the hypergeometric function, $w=-\exp(x/a)$, $f=\sqrt{E/\Delta}$, $g=[4V_0/\Delta-(1/4)]^{1/2}$, and $s=\sqrt{E/\Delta}$, where $\Delta=\hbar^2/(2ma^2)$. The exact QMF and the quantum potential in the complex plane can be calculated by making an analytic continuation of this wave function from x to z. Here, we calculated complex powers using the principal value of the argument of a complex number z by specifying that $-\pi<\arg(z)\leqslant\pi$. From $w=-\exp(z/a)$, the exponential function is periodic with period $2\pi i$ along the y direction. The argument function $\arg(z)$ has a branch cut discontinuity in the complex plane running from $-\infty$ to 0, so this leads to the discontinuity of the exact QMF along $y=\pm\pi i,\pm 3\pi i,\pm 5\pi i,\ldots$ for $x<0$. Similarly, the analytic continuation of the Eckart potential reveals periodicity along the direction of the imaginary axis. For example, this potential gives the same value for $z=x+iy$ and $z=x+i(y+2\pi)$. Therefore, for this problem, the complex plane can be divided into an infinite number of zones with the boundaries $y=\pm\pi i,\pm 3\pi i,\pm 5\pi i,\ldots$.

The quantum trajectories can be obtained by solving the equations of motion given in Eqs. (36)–(38). However, we need to choose appropriate initial conditions. In this section, the quantum trajectories will be determined by two methods: either *forward* or *backward* integrations. For the forward integration, the exact QMF calculated from the scattering wave function will be used as the initial condition to determine the quantum trajectories. For the backward integration, the *asymptotic* QMF in the transmission region will be used as

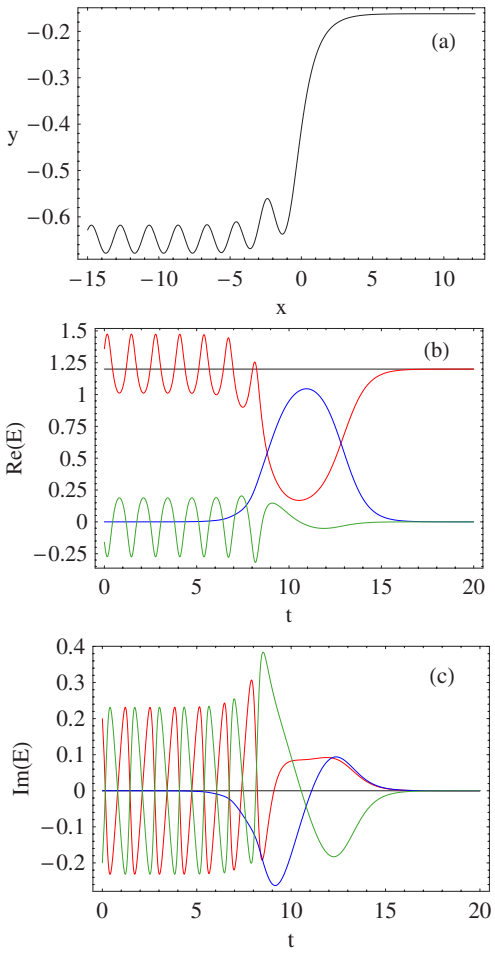

FIG. 11. (Color online) Analysis of quantum trajectory for $E=1.2$, $V_0=1$: (a) Quantum trajectory starting from the initial position at $z=-15-\pi i/5$. Time dependence of the total energy (black), the kinetic energy (red), the classical potential (blue), and the quantum potential (green) along the quantum trajectory: (b) Real part; (c) imaginary part. The trajectory was integrated from $t=0$ to $t=20$.

the initial condition to determine the quantum trajectories by integrating the equations of motion *backwards*. In addition, the relevant physical quantities will be used in the dimensionless units: $\bar{z}=z/a$, $\bar{p}=p/(\hbar/a)$, $\bar{t}=t/(ma^2/\hbar)$, $\bar{E}=E/2\Delta$, and $\bar{V_0}=V_0/2\Delta$. We will denote the value of a given dimensionless physical quantity with the same symbol as the quantity itself.

1. Forward integration

Figures 9 and 10 show the quantum trajectories and the corresponding complex-valued total potential with $E=1.2$ and $V_0=1$. We numerically integrate the equations of motion with the exact initial QMF from $t=0$ to $t=15$ by starting the integration in the reflection region [38]. We chose the initial positions with the same real part but with different imaginary parts: $z=-7+i(\pi/10+k\pi/5)$, where $k=0,\pm1,\pm2,\ldots$. Because the motion of the particle is governed by the complex-valued total force, the quantum trajectories and the real and

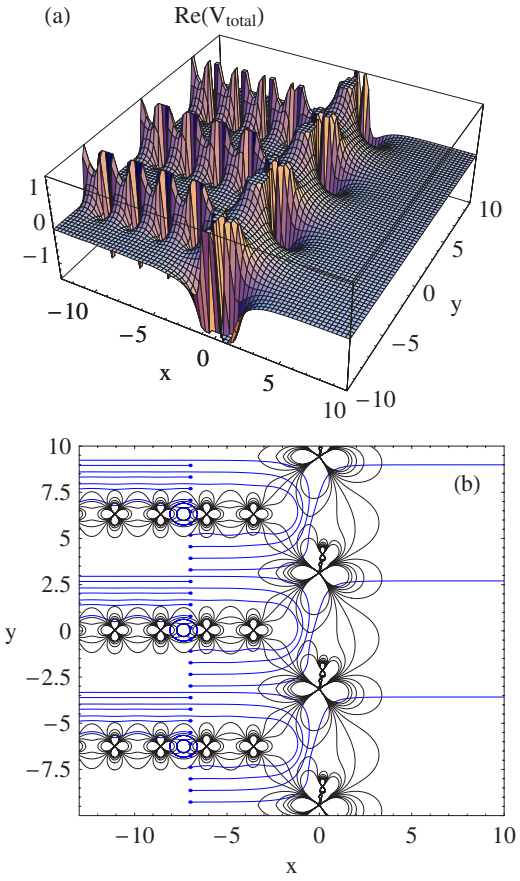

FIG. 12. (Color online) Forward integration for $E=0.8$, $V_0=1$: (a) Real part of the total potential; (b) quantum trajectories (blue curves) and the contour map of the real part of the total potential (black curves). The initial positions are shown as blue dots.

the imaginary parts of the total potential are shown in Figs. 9 and 10. From these figures, we can see the periodicity of the total potential along the direction of the imaginary axis and the different structure of the total potential between the reflection and the transmission regions. The classical potential only has singularities along the imaginary axis; hence, the singularities and the "channel" structure on the left side of the imaginary axis are contributed by the quantum potential. In Figs. 9(b) and 10(b), some particles start their motion on the *left side* of the barrier, and then they pass the potential to the transmission region. In addition, some particles launched from the initial positions move toward the left. In particular, there are some loops or closed trajectories on the "walls" of the "channel" structure.

In Fig. 11, we present the total energy, the kinetic energy, the classical potential, and the quantum potential for the trajectory launched at $z=-15-\pi i/5$ from $t=0$ to $t=20$. For this trajectory, the particle starts its oscillatory motion from the left side of the potential and then passes the barrier to the transmission region. The quantum trajectory in the complex plane satisfies the stationary-state QHJE given in Eq. (35), so the sum of the *complex-valued* kinetic energy, the *complex-valued* classical, and the *complex-valued* quantum potentials is conserved and it is equal to the *real-valued* total energy. In this figure, we can see that the kinetic energy and the quan-

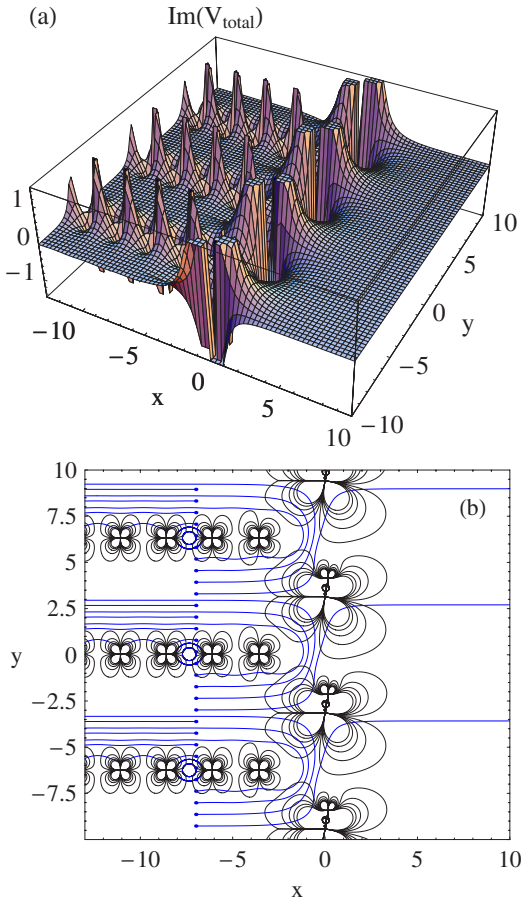

FIG. 13. (Color online) Forward integration for $E=0.8$, $V_0=1$: (a) Imaginary part of the total potential; (b) quantum trajectories (blue curves) and the contour map of the imaginary part of the total potential (black curves). The initial positions are shown as blue dots.

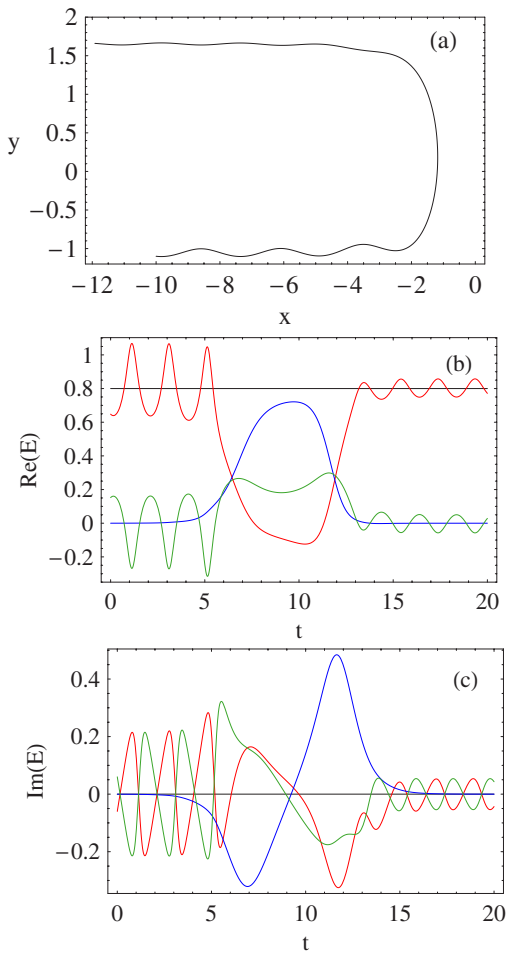

FIG. 14. (Color online) Analysis of quantum trajectory for $E=0.8$, $V_0=1$: (a) Quantum trajectory starting from the initial position at $z=-10-7\pi i/20$. Time dependence of the total energy (black), the kinetic energy (red), the classical potential (blue), and the quantum potential (green) along the quantum trajectory: (b) Real part; (c) imaginary part. The trajectory was integrated from $t=0$ to $t=20$.

tum potential on the left side of the barrier compensate each other and the classical potential is equal to zero there. After the particle passes the barrier, the classical and the quantum potentials gradually become zero and finally all the total energy is concentrated into the *real-valued* kinetic energy.

Figures 12 and 13 show the quantum trajectories and the corresponding complex-valued total potential for the tunneling energy $E=0.8$ and $V_0=1$. We numerically integrate the equations of motion with the exact initial QMF from $t=0$ to $t=20$ by starting the integration in the reflection region. The initial positions were $z=-7+i(\pi/20+k\pi/5)$, where $k=0,\pm1,\pm2,\ldots$. In Figs. 12(b) and 13(b), fewer trajectories link the left and right regions of these figures than those for $E=1.2$. Additionally, some particles move toward the barrier, but they rebound instead of passing to the transmission region. Similarly, some particles launched from the initial positions move to the left side and some closed trajectories are imbedded in the "walls" of the "channel" structure. In Fig. 14, we present the total energy, the kinetic energy, the classical potential, and the quantum potential for the trajectory launched from the position $z=-10-7\pi i/20$. For this trajectory, the particle starts its oscillatory motion from the left side of the barrier and then bounces back to the reflection region. When the particle is far from the barrier, the classical potential approaches zero and the kinetic energy and the quantum potential compensate each other. Again, the total energy is conserved.

2. Backward integration

We know that the scattering wave function approaches e^{ikx} asymptotically when x tends to ∞ along the real axis. Hence, the asymptotic form of the scattering wave function in the transmission region can be used to determine the initial conditions for the trajectory. Then, we can numerically integrate the equations of motion *backwards* from the transmission region. Thus, substituting this asymptotic form into the definition of the stationary-state QMF gives $\bar{p}(x)=\hbar k$. Then, this equation can be used as the initial condition for the equations of motion. Although the QMF tends to the constant $\hbar k$ asymptotically for large x along the real axis, it actually approaches the same constant in the transmission region on the complex plane provided that the position is far enough away

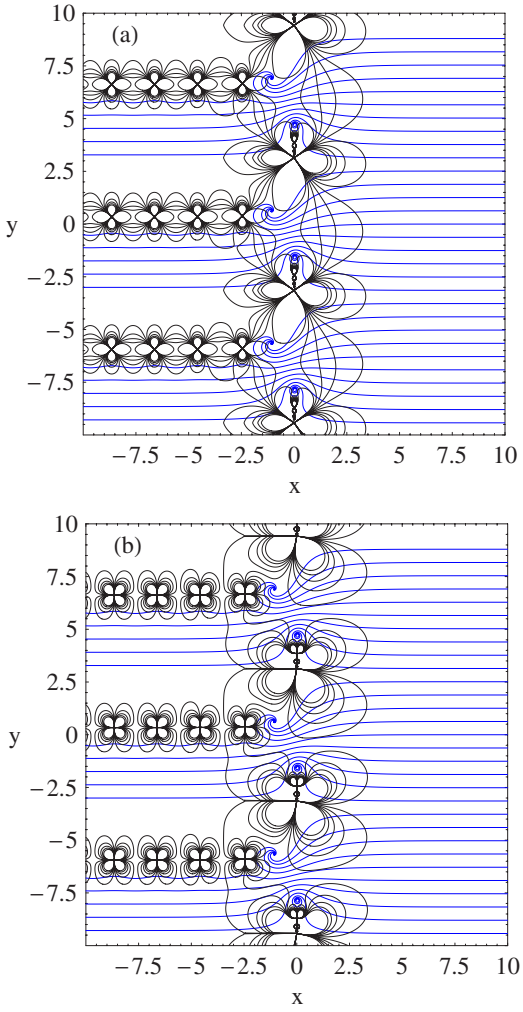

FIG. 15. (Color online) Backward integration for $E=1.2$, $V_0=1$: Quantum trajectories (blue curves) and the contour map of the total potential (black curves): (a) Real part; (b) imaginary part.

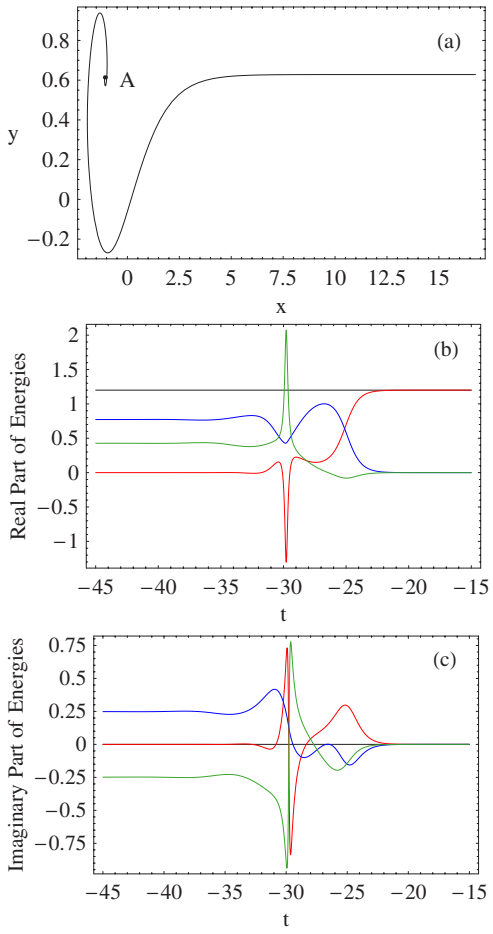

FIG. 16. (Color online) Analysis of quantum trajectory using backward integration for $E=1.2$, $V_0=1$: (a) Quantum trajectory determined backwards with the initial position $z=40+(\pi/5)i$. Time dependence of the total energy (black), the kinetic energy (red), the classical potential (blue), and the quantum potential (green) along the quantum trajectory: (b) Real part; (c) imaginary part. The trajectory was integrated from $t=0$ to $t=-45$.

from the imaginary axis. We can also apply the Möbius integrator [37] to the Riccati-type stationary-state QHJE in Eq. (35) to determine the approximate initial QMF off the real axis. It is found that the constant $\hbar k$ is an excellent choice for the initial QMF in the transmission region.

Figure 15 shows the quantum trajectories and the corresponding contour map of the complex-valued total potential with $E=1.2$ and $V_0=1$. The complex-valued total potential for $E=1.2$ has been shown in Figs. 9(a) and 10(a). We numerically integrate the equations of motion with the initial condition $\bar{p}(z)=\hbar k$ *backwards* from $t=0$ to $t=-40$ by starting the integration in the transmission region. The initial positions were $z=40+k\pi i/5$, where $k=0,\pm1,\pm2,\ldots$. Similarly, we find that some trajectories link the left and right regions of these figures. Other trajectories are traced back to positions near the barrier region and spiral into "attractors."

In Fig. 16, we present the total energy, the kinetic energy, the classical potential, and the quantum potential for the trajectory integrated backwards from the initial position $z=40+(\pi/5)i$ for $E=1.2$. The trajectory is traced back to the attractor. From the viewpoint of the particle's forward motion, it starts at the position of the attractor and then slides down the potential to the transmission region. We note from this figure that the kinetic energy equals zero when the particle is located at the position of the attractor. In addition, the kinetic energy is almost equal to zero from $t=-45$ to $t=-35$, the sum of the real parts of the classical and the quantum potentials is equal to the *real-valued* total energy, and the imaginary parts of the classical and the quantum potentials cancel each other. Then, some of the total potential energy is transferred into the kinetic energy to initiate the particle's motion. The final kinetic energy arises from the initial total potential energy, and the total energy is conserved all the time.

The quantum trajectories and the corresponding complex-valued total potential with the tunneling $E=0.8$ and $V_0=1$ are shown in Fig. 17. The complex-valued total potential for $E=0.8$ has been shown in Figs. 12(a) and 13(a). The initial positions were $z=40+i(\pi/10+k\pi/5)$, where $k=0,\pm1,\pm2,\ldots$. We note from these figures that most quantum trajectories are traced from the transmission region back to the attractors in the barrier region. Additionally, the trajec-

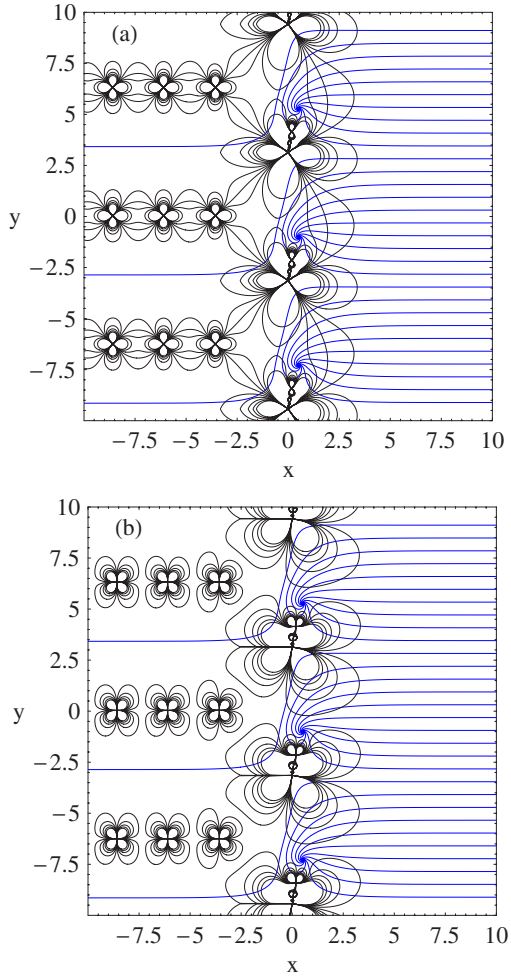

FIG. 17. (Color online) Backward integration for $E=0.8$, $V_0=1$: Quantum trajectories (blue curves) and the contour map of the total potential (black curves): (a) Real part; (b) imaginary part.

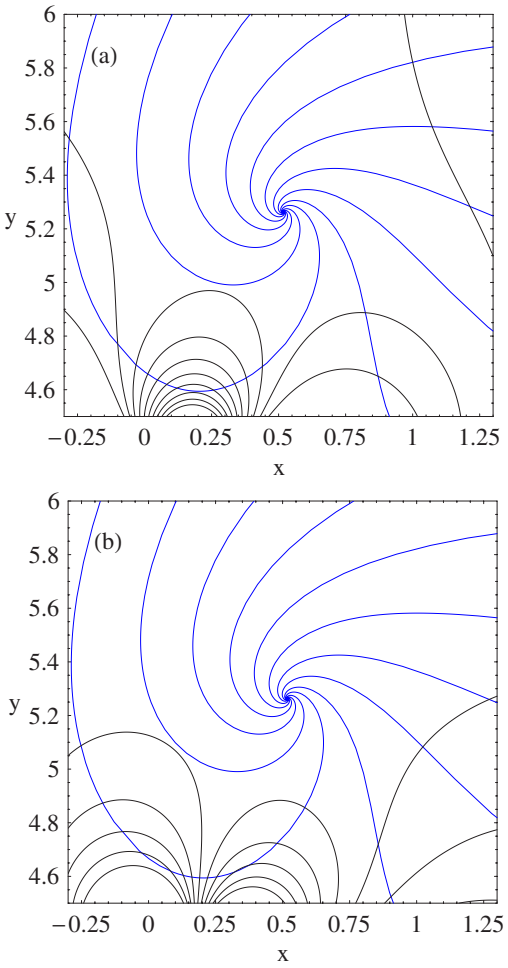

FIG. 18. (Color online) Backward integration for $E=0.8$, $V_0=1$: quantum trajectories (blue curves) near an attractor and the contour map of the real part (a) and the imaginary part (b) of the total potential.

tories spiraling into the attractor at $z=0.518+5.262i$ are shown in Fig. 18.

VI. SUMMARY AND CONCLUSIONS

In this study, a unified description of complex quantum trajectories was presented. In the quantum Hamilton-Jacobi formalism, the quantum momentum function is extended to the complex space and the energy eigenvalues can be determined by the quantum action variable. Similarly, the complex quantum trajectory can be obtained through the guidance equation by extending the position coordinate to the complex space. Then, the equations of motion for complex quantum trajectories for time-dependent and time-independent problems were derived in the framework of the quantum Hamilton-Jacobi formalism.

For time-dependent problems, complex quantum trajectories and the concept of isochrone were demonstrated by two exactly solvable systems: the free Gaussian wave packet and the coherent state in the harmonic potential. We also showed that the particles may exhibit complicated motions in the complex plane and that the information transported by the particles launched from isochrones can be used to synthesize the time-dependent wave function.

For time-independent problems, difficulties that arise when determining complex quantum trajectories for stationary states were discussed. Subsequently, we determined the complex quantum trajectories for the Eckart potential using two methods: the forward and the backward integrations. In the forward integration, we used the exact initial condition in the reflection region to solve the equations of motion. The total potential (the sum of the classical and the quantum potentials) calculated from the exact scattering wave function is periodic along the direction of the imaginary axis and reveals a complicated channel structure in the reflection region. Some trajectories link the reflection and transmission regions, and some form closed loops imbedded in the walls of the channel structure. Some particles start their motion from the left side of the barrier and then bounce back to the reflection region. In the backward integration, the asymptotic quantum momentum function in the transmission region was used as the initial condition to numerically solve the equations of motion backwards. Some trajectories in the transmission region were found to spiral into a set of attractors in the

barrier region. The sum of the complex-valued kinetic energy, classical potential, and quantum potential is equal to the real-valued scattering energy. We also described the time dependence of these energies along several trajectories.

In this study, we have presented a unified treatment of complex quantum trajectories in the quantum Hamilton-Jacobi formalism. For time-dependent problems, we analytically studied exactly solvable systems to understand how the information transported by the particles launched from isochrones can be used to synthesize the time-dependent wave function. Tannor and co-workers recently proposed a computational method to obtain the complex quantum trajectories and the wave function [22]. For time-independent problems, complex quantum trajectories have been determined for the free particle, the potential step, the potential barrier, the harmonic potential, and the hydrogen atom from the exact analytical wave functions [14–21]. Here, we determined the complex quantum trajectories by numerically integrating the equations of motion for the Eckart potential. In addition, we recently proposed an accurate computational method for the stationary-state version of the QHJE for one-dimensional bound state and scattering problems [12,13]. Thus, our present paper complements these studies and provides a unified description for complex quantum trajectories for one-dimensional problems under the framework of the quantum Hamilton-Jacobi formalism. In the future, the computational method to determine the appropriate initial QMF for complex quantum trajectories for stationary states needs to be developed. Additionally, complex quantum trajectories and relevant computational methods for multidimensional problems deserve further investigation.

ACKNOWLEDGMENTS

We thank Brad Rowland and Julianne David for helpful comments and the Robert Welch Foundation for their financial support of this research.

[1] D. Bohm, Phys. Rev. **85**, 166 (1952).
[2] A. S. Sanz, F. Borondo, and S. Miret-Artés, Phys. Rev. B **61**, 7743 (2000).
[3] Z. S. Wang, G. R. Darling, and S. Holloway, J. Chem. Phys. **115**, 10373 (2001).
[4] C. L. Lopreore and R. E. Wyatt, Phys. Rev. Lett. **82**, 5190 (1999).
[5] R. E. Wyatt, *Quantum Dynamics with Trajectories: Introduction to Quantum Hydrodynamics* (Springer, New York, 2005).
[6] F. S. Mayor, A. Askar, and H. A. Rabitz, J. Chem. Phys. **111**, 2423 (1999).
[7] P. R. Holland, *The Quantum Theory of Motion: An Account of the de Broglie-Bohm Causal Interpretation of Quantum Mechanics* (Cambridge University Press, New York, 1993).
[8] R. A. Leacock and M. J. Padgett, Phys. Rev. Lett. **50**, 3 (1983).
[9] R. A. Leacock and M. J. Padgett, Phys. Rev. D **28**, 2491 (1983).
[10] R. S. Bhalla, A. K. Kapoor, and P. K. Panigrahi, Am. J. Phys. **65**, 1187 (1997).
[11] R. S. Bhalla, A. K. Kapoor, and P. K. Panigrahi, Mod. Phys. Lett. A **12**, 295 (1997).
[12] C.-C. Chou and R. E. Wyatt, J. Chem. Phys. **125**, 174103 (2006).
[13] C.-C. Chou and R. E. Wyatt, Phys. Rev. E **74**, 066702 (2006).
[14] M. V. John, Found. Phys. Lett. **15**, 329 (2002).
[15] C.-D. Yang, Ann. Phys. (N.Y.) **319**, 339 (2005).
[16] C.-D. Yang, Ann. Phys. (N.Y.) **319**, 444 (2005).
[17] C.-D. Yang, Int. J. Quantum Chem. **106**, 1620 (2006).
[18] C.-D. Yang, Chaos, Solitons Fractals **30**, 342 (2006).
[19] C.-D. Yang, Ann. Phys. (N.Y.) **321**, 2876 (2006).
[20] C.-D. Yang, Chaos, Solitons Fractals **32**, 312 (2007).
[21] C.-D. Yang, Chaos, Solitons Fractals **33**, 1073 (2007).
[22] Y. Goldfarb, I. Degani, and D. J. Tannor, J. Chem. Phys. **125**, 231103 (2006).
[23] B. A. Rowland and R. E. Wyatt, J. Phys. Chem. (to be published).
[24] R. E. Wyatt and B. A. Rowland, J. Chem. Phys. (to be published).
[25] W. H. Miller and T. F. George, J. Chem. Phys. **56**, 5668 (1972).
[26] T. F. George and W. H. Miller, J. Chem. Phys. **56**, 5722 (1972).
[27] T. F. George and W. H. Miller, J. Chem. Phys. **57**, 2458 (1972).
[28] E. J. Heller, J. Chem. Phys. **62**, 1544 (1975).
[29] D. Huber and E. J. Heller, J. Chem. Phys. **87**, 5302 (1987).
[30] D. Huber, E. J. Heller, and R. G. Littlejohn, J. Chem. Phys. **89**, 2003 (1988).
[31] M. Boiron and M. Lombardi, J. Chem. Phys. **108**, 3431 (1998).
[32] D. J. Tannor, *Introduction to Quantum Mechanics: A Time-Dependent Perspective* (University Science Books, Sausalito, 2007).
[33] C. J. Trahan, K. H. Hughes, and R. E. Wyatt, J. Chem. Phys. **118**, 9911 (2003).
[34] P. L. Hagelstein, S. D. Senturia, and T. P. Orlando, *Introductory Applied Quantum and Statistical Mechanics* (John Wiley & Sons, Hoboken, 2004).
[35] I. I. Gol'dman and V. D. Krivchenkov, *Problems in Quantum Mechanics* (Dover, Mineola, 1993).
[36] Z. Ahmed, Phys. Rev. A **47**, 4761 (1993).
[37] J. Schiff and S. Shnider, SIAM (Soc. Ind. Appl. Math.) J. Numer. Anal. **36**, 1392 (1999).
[38] In Sec. V B, we used the built-in function NDSolve in MATHEMATICA 5.0 to find the numerical solutions of the equations of motion given by Eqs. (36)–(38) and we set WorkingPrecision to be MachinePrecision, Method to be StiffnessSwitching, MaxSteps to be 100 000, and MaxStepSize to be 0.01.